POST-ICA PHASE DE-NOISING FOR RESTING-STATE COMPLEX-VALUED FMRI DATA

Li-Dan Kuang [1], Qiu-Hua Lin [1], Xiao-Feng Gong [1], Fengyu Cong [2,3], and Vince D. Calhoun[4,5]

[1] School of Information and Communication Engineering, Dalian University of Technology, Dalian 116024, China
qhlin@dlut.edu.cn
[2] Department of Biomedical Engineering, Dalian University of Technology, China
[3] Department of Mathematical Information Technology, University of Jyvaskyla, Finland
[4] The Mind Research Network, Albuquerque, NM 87106, USA
[5] Department of Electrical and Computer Engineering, University of New Mexico, Albuquerque, NM 87131, USA

ABSTRACT

Magnitude-only resting-state fMRI data have been largely investigated via independent component analysis (ICA) for exacting spatial maps (SMs) and time courses. However, the native complex-valued fMRI data have rarely been studied. Motivated by the significant improvements achieved by ICA of complex-valued task fMRI data than magnitude-only task fMRI data, we present an efficient method for de-noising SM estimates which makes full use of complex-valued resting-state fMRI data. Our two main contributions include: (1) The first application of a post-ICA phase de-noising method, originally proposed for task fMRI data, to resting-state data, which recognizes voxels within a specific phase range as desired voxels. (2) A new phase range detection strategy for a specific SM component based on correlation with its reference. We continuously change the phase range within a larger range, and compute a set of correlation coefficients between each de-noised SM and its reference. The phase range with the maximal correlation determines the final selection. The detected results by the proposed approach confirm the correctness of the post-ICA phase de-noising method in the analysis of resting-state complex-valued fMRI data.

***Index Terms*—**Independent component analysis (ICA), complex-valued fMRI data, resting-state fMRI data, phase de-noising, phase range detection

1. INTRODUCTION

Resting-state functional magnetic resonance imaging (fMRI) data have attracted widespread interest in recent years since they are easily collected especially for cognitively-impaired patients in contrast to task fMRI data [1], and reflect spontaneous neuronal activity [2, 3]. With the aid of model-based methods or data-driven methods, resting-state fMRI data have found successful applications to brain function and diseases study. This study focuses on a widely used data-driven method called independent component analysis (ICA), which is capable of extracting spatial maps (SMs) and time courses (TCs) from fMRI data without any knowledge about the data [4-8]. ICA-separated SMs provide spatially localized connectivity networks containing correlated activity [9], and the TCs are frequently exploited for functional network connectivity (FNC), a measure of between network connectivity [5-8, 10, 11]. FNC has been shown to be significantly different for healthy controls and patients, e.g., schizophrenia [5, 6], Alzheimer [7], major depressive disorder [8], and bipolar disorder [6] among others.

Resting-state fMRI data are initially acquired as complex-valued image pairs including magnitude and phase information [12-16]. However, to our best knowledge, existing ICA analysis have studied only magnitude resting fMRI data. This study aims to explore ICA of full resting-state complex-valued data, in an effort to extract improved components compared to magnitude-only fMRI data. Our motivation comes from the results obtained from ICA of complex-valued task fMRI data with a proper de-noising strategy. Note phase de-noising is essential for the analysis of complex-valued fMRI data, as phase fMRI data are much noisier than magnitude fMRI data [15, 16]. A complex-valued ICA method with pre-ICA phase de-noising (utilizing observed phase images to identify and remove noisy voxels in fMRI data) achieved higher sensitivity and specificity than magnitude-only ICA methods [14, 17, 18]; and the complex-valued method using post-ICA phase de-noising (exploiting the SM phase information to identify and remove noisy voxels in ICA estimates) detected more of the desired

BOLD-related voxels than pre-ICA de-noising and extracted more contiguous and reasonable activations than a magnitude-only method for task-related (139%) and default mode (331%) SMs [16]. This shows the potential to improve ICA of resting-state fMRI data by utilizing complex-valued data and a proper phase de-noising method.

In this study, we utilize full resting-state complex-valued fMRI data using a post-ICA phase de-noising method [16]. Since this post-ICA phase de-noising method was originally proposed for task fMRI data, and recognized the voxels with phase values within a specific range $\pm\Delta\varphi$ (e.g., $\Delta\varphi=\pi/4$) as the desired BOLD-related voxels, this study mainly examines two aspects: (1) If the existing post-ICA phase de-noising method can be directly applied to the resting-state fMRI data; (2) If the specific range $\Delta\varphi=\pi/4$ is efficient for resting-state fMRI data. In order to answer these questions, we propose a new phase range detection strategy based on correlation with prior SM references. The detected results by this new strategy confirm the correctness of the post-ICA phase de-noising method in the analysis of resting-state complex-valued fMRI data.

2. POST-ICA PHASE DE-NOISING

Assume there are N components for ICA to estimate; $\mathbf{s}_i$ ($i=1,\dots,N$) is an SM component estimated by ICA and adjusted to remove phase ambiguity by maximizing the real-part power of its corresponding TC [16]. Let $\mathbf{s}_{i,\text{phase}}$ denote its phase image, $\mathbf{s}_{i,\text{phase}}(l)$ the phase value of voxel l, l the voxel index ($l=1,\dots,L$), and L the total number of the brain voxels obtained by flattening the volume image data. The range of $\mathbf{s}_{i,\text{phase}}(l)$ is $[-\pi,\pi]$ (without wrapping).

The post-ICA phase de-noising method classifies the whole voxels of $\mathbf{s}_i$ into two categories according to their phase values, the BOLD-related voxels and the unwanted voxels (caused probably by large vessels, physiologic noise and motion) [16]:

$$\text{voxel}(l)=\begin{cases}\text{BOLD-related}, & \textit{if } \mathbf{s}_{i,\text{phase}}(l)\in\pm\Delta\varphi\\ \text{unwanted}, & \textit{otherwise}\end{cases} \tag{1}$$

where voxel(l) denotes the voxel of index l in $\mathbf{s}_i$; $\pm\Delta\varphi$ denotes the phase range of the desired BOLD-related voxels, and $\Delta\varphi=\pi/4$ for task fMRI data.

For de-noising ICA-estimated SMs in a single-subject analysis, a binary phase mask for subject p is constructed as [16]:

$$\text{BM1}^p(\Delta\varphi)=\begin{cases}1, & \textit{if } \mathbf{s}^p_{i,\text{phase}}(l)\in\pm\Delta\varphi\\ 0, & \textit{otherwise}\end{cases} \tag{2}$$

By masking a single-subject SM estimate with $\text{BM1}^p(\Delta\varphi)$, the goal of SM de-noising is achieved.

3. NEW PHASE RANGE DETECTION METHOD

Considering the phase range $\pm\Delta\varphi$ is an empirical choice, e.g., $\Delta\varphi=\pi/4$ is suitable for task fMRI data, we propose a precise phase range detecting approach for a specific SM component based on correlation with its SM reference. As the phase range of the desired BOLD-related voxels may be larger than $\pm\pi/4$, we continuously change the phase range within a larger range $\Delta\varphi\in(0,\pi/2]$, and then calculate a set of correlation coefficients between each de-noised SM and its reference. The phase range corresponding to the maximal correlation coefficient is the final selection for de-noising this SM component:

$$\Delta\varphi=\underset{\Delta\varphi\in(0,\pi/2]}{\arg\max}\ \text{corr}\left\{\left|\mathbf{s}_i\cdot\text{BM1}^p(\Delta\varphi)\right|,\mathbf{s}_{i,ref}\right\} \tag{3}$$

where $\mathbf{s}_{i,ref}$ denotes a magnitude-only prior SM reference for $\mathbf{s}_i$, which can be generated from spatial networks consistently found in previous studies [20] or from the available atlases including Brodmann areas and functional areas using WFUPickAtlas [23]; "$\mathbf{s}_i\cdot\text{BM1}^p(\Delta\varphi)$" de-noised $\mathbf{s}_i$ with phase range $\pm\Delta\varphi$, "$\cdot$" the dot product, "$|\ |$" magnitude calculation, and "corr" correlation computation.

A practical implementation for the proposed approach is as follows: let $\Delta\varphi=k\pi/2K, k=1,\dots K$. Then we generate K phase ranges for detecting, i.e., $\pm\pi/2K,\dots, \pm\pi/2$. The larger K is, the more precise the detected phase range is. In this study, we set K=32.

With a newly detected phase range, a component-specific mask can be constructed using Eq. (2).

4. EXPERIMENTS AND RESULTS

4.1. Resting-State fMRI Data

The resting-state complex-valued fMRI data were collected from 24 healthy controls recruited by University of New Mexico, with written subject consents. FMRI scans were acquired using a 3.0 Tesla Siemens Allegra scanner, equipped with 40 mT/m gradients and a standard quadrature head coil. The functional scan was acquired using gradient-echo echo-planar imaging with the following parameters: TR = 1.86 s, TE = 27 ms, field of view = 24 cm, acquisition matrix = 64 × 64, flip angle = 70°, slice thickness =3 mm, slice gap = 1 mm. During the scan, all participants were instructed to rest quietly in the scanner, keep their eyes open without sleeping and not to think of anything in particular. Data preprocessing was performed using the SPM software package (http://www.fil.ion.ucl.ac.uk/spm). In order to avoid T1 magnetization effects, the first several dummy scans were excluded and 146 resting state scans were used for analysis.

After motion correction, the functional images were normalized into Montreal Neurological Institute standard space. Following spatial normalization, the data were slightly sub-sampled to 3 × 3 × 3 mm^3, resulting in 53 × 63 × 46 voxels. Both the real and imaginary images were spatially smoothed with a 10 mm^3 full width half-maximum (FWHM) Gaussian kernel.

4.2. Three Components of Interest

There are a large number of components in resting-state fMRI data. We changed N from 40 to 80, and found that the separation performance for N=60 was better. Therefore, we used entropy bound minimization (EBM) algorithm [19], an efficient complex-valued ICA algorithm, to first separate 60 components, and then selected three components of interest as examples for evaluation. The three selected components are a medial visual component, the default mode network (DMN) component, and a sensorimotor component. Their magnitude-only SM references are available in [20].

For comparison, we also performed magnitude-only analysis using the widely-used Infomax algorithm [21] with N = 60. Since we used $|Z| > 0.5$ as the threshold of z-scored SM estimates for our method, we provided two groups of Infomax results for magnitude-only analysis: (1) $|Z| > 0.5$; (2) $|Z| > 2.5$, as 2.5 is a typical threshold for reliably removing noisy voxels in SMs for magnitude-only method. We calculated Pearson correlation coefficient ρ between magnitudes of SM estimates with their corresponding references to evaluate the performance.

4.3. Results of Phase Range Detection

For a single-subject of fMRI data, we first obtained the SM estimates for three components of interest, i.e., the medial visual component, the DMN component, and the sensorimotor component, by using the prior SM references, and then detected the phase ranges $\pm\Delta\varphi$ of the desired BOLD-related voxels for each component, according to Eq. (3). Fig. 1 includes the results for 24 subjects. We can observe that majority of the detected phase ranges are smaller than $\pi/4$, which was derived for task fMRI data based on a criterion of TC real-part power maximization [16]. We examine detailed information for 5 subjects (subjects 1, 3, 4, 16, 20, who showed a larger phase range than $\pi/4$) in terms of the number of voxels inside and outside of the phase range $\pm\pi/4$ in Table 1. We find that there were only very few voxels whose phase values were larger than $\pm\pi/4$ (maximum 3.49%, minimum 0.04%), though the detected phase range was larger than $\pm\pi/4$. This suggests that $\pm\pi/4$ is also suitable for de-noising resting-state complex-valued fMRI data.

4.4. Results from Single-Subject Analyses

We showed the results of three components of interest from one exampling subject (subject 2) in Fig. 2. We compared the de-noised SMs using phase range $\pm\pi/4$ and the detected phase range $\pm\Delta\varphi$, in addition to the SM estimates before phase de-noising, the SM references for the medial visual component, the DMN component, and the sensorimotor component. The correlation coefficients of de-noised SMs with the SM references are also shown in Fig. 2. The phase de-noising effects can be readily observed from columns 2 and 3. Prior to phase de-noising (column 2), SM estimates contained many unwanted voxels with both larger and lower amplitudes than the desired BOLD-related voxels. After phase de-noising, the noisy voxels were largely eliminated. When comparing the results for two phase ranges, see column 3 ($\pm\pi/4$) and column 4 (our detected much smaller phase ranges: $\pm3\pi/64$, $\pm\pi/16$, and $\pm\pi/8$), they look highly similar, though the proposed method obtained higher correlation coefficients. Therefore, the phase range $\pm\pi/4$ is proper for the resting-state fMRI data.

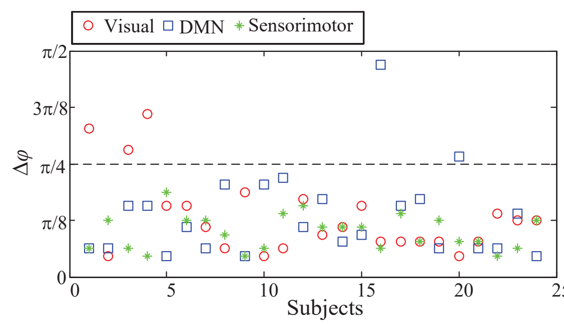

Fig. 1. The phase ranges detected for three components of interest (the medial visual component, the DMN component, and the sensorimotor component) by the proposed method from 24 subjects of resting-state complex-valued fMRI data.

Table 1. The number of voxels inside and outside of the phase range $\pm\pi/4$, their difference, and the ratio of the difference to the total voxels detected by the proposed method ($\pm\Delta\varphi$) for 5 subjects (subject 1, 3, 4, 16, 20). "Subject" is shorted as "S".

	Visual			DMN	
	S1	S3	S4	S16	S20
$\pm\Delta\varphi$	9356	8691	10606	10758	11018
$\pm\pi/4$	9261	8678	10583	10383	11014
difference	95	13	23	375	4
ratio	1.02%	0.15%	0.22%	3.49%	0.04%

4.5. Comparison with Magnitude-only Method

Fig. 3 includes magnitude-only results estimated by real-valued Infomax (N = 60) using two difference thresholds:

|Z| > 0.5 and |Z| > 2.5, with comparison to the de-noised SMs using our detected phase range (the same as those shown in the last column of Fig. 2). The Infomax results with |Z| > 0.5 included more unwanted voxels than those with |Z| > 2.5, thus had relatively lower correlation coefficients with the references. The de-noised SMs obtained by the proposed method not only yielded higher correlation coefficients, but also detected more contiguous and reasonable activations. Table 2 displays quantitative comparison of complex-valued method and magnitude-only method (|Z| > 2.5) in terms of number of total voxels, voxels inside and outside of the references for three SM estimates. We can find that complex-valued method detected 6 times as many as magnitude-only method for total voxels, and 3~4 times for voxels inside the references. As for the large number of voxels outside the references, which were detected by complex-valued method, most of them were expected to be activated. For example, complex-valued analysis extracted additional voxels in the occipital pole visual areas for the medial visual component [20], the medial prefrontal cortex and posterior cingulate cortex for the DMN component [22], and primary motor area for the sensorimotor component.

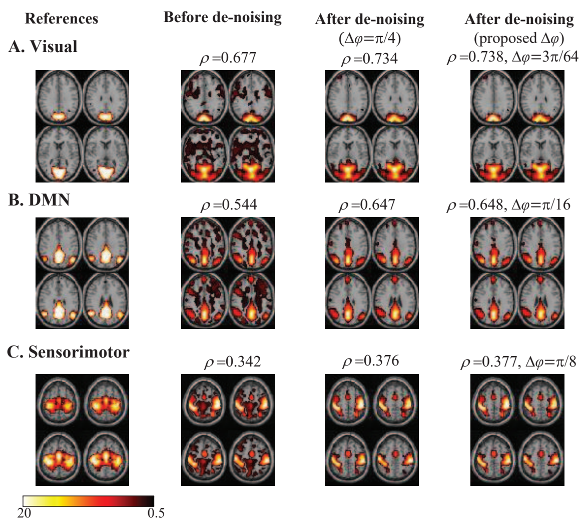

Fig. 2. De-noised SMs (|Z| > 0.5) using phase range $\pm\pi/4$ and our detected phase range $\pm\Delta\varphi$ for subject 2. (A) The media visual component. (B) The DMN component. (C) The sensorimotor component. SM estimates before phase de-noising, SM references and correlation coefficients of de-noised SMs with the SM references are also shown.

5. CONCLUSION

Post-ICA phase de-noising was originally proposed for task complex-valued fMRI data with a derived phase range $\pm\pi/4$. In this study, we applied post-ICA phase de-noising to resting-state complex-valued fMRI data. In the meantime, we proposed a new phase range detection strategy for a specific SM component based on correlation with its prior SM reference. Experimental results from 24 subjects show that the proposed method can find more precise phase range, thus can be used separately. The phase range $\pm\pi/4$ is correct and general for both resting-state and task fMRI data. Compared with magnitude-only ICA, complex-valued method can detect more contiguous and reasonable activations.

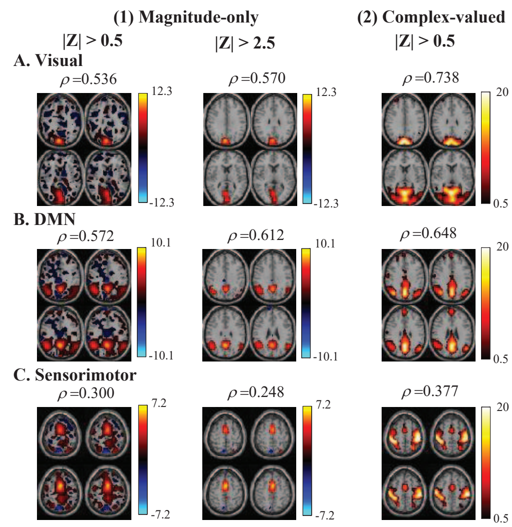

Fig. 3. Comparison of complex-valued analysis using our method (|Z| > 0.5) and magnitude-only analysis using Infomax (|Z| > 0.5 and |Z| > 2.5) for subject 2. (A) The media visual component. (B) The DMN component. (C) The sensorimotor component. Correlation coefficients with the SM references are shown.

Table 2. Number of total voxels, voxels inside and outside of the references for three SMs detected by complex-valued method and magnitude-only method (|Z| > 2.5) for subject 2.

		Total	Inside reference	Outside reference
Visual	Complex	8744	4011	4733
	Magnitude	1461	1219	242
DMN	Complex	10936	5526	5410
	Magnitude	1770	1475	295
Sensori-motor	Complex	9736	2925	6811
	Magnitude	1532	718	814

6. ACKNOWLEDGEMENT

This work was supported by National Natural Science Foundation of China under Grants 61379012, 61105008, 61331019 and 81471742, NSF grants 0840895 and 0715022, NIH grants R01EB005846 and 5P20GM103472, the Fundamental Research Funds for the Central Universities (China, DUT14RC(3)037), and China Scholarship Council.

7. REFERENCES

[1] X.W. Song, Z.Y. Dong, X.Y .Long, S.F .Li, X.N. Zuo, C.Z. Zhu, et al, "Rest: a toolkit for resting-state functional magnetic resonance imaging data processing," *Plos One*, vol. 6, no. 9, pp. e25031, September 2011.

[2] N.K. Logothetis, J. Pauls, M. Augath, T. Trinath, and A. Oeltermann, "Neurophysiological investigation of the basis of the fMRI signal," *Nature*, vol. 412, no. 6843, pp. 150-157, July 2001.

[3] A. Rauch, G. Rainer, and N.K. Logothetis, "The effect of a serotonin-induced dissociation between spiking and perisynaptic activity on BOLD functional MRI," *Proceedings of the National Academy of Sciences*, vol. 105, no. 18, pp. 6759-6764, May 2008.

[4] V. Kiviniemi, J.-H. Kantola, J. Jauhiainen, A. Hyvärinen, and O. Tervonen, "Independent component analysis of nondeterministic fMRI signal sources," *NeuroImage*, vol. 19, no. 2, pp. 253-260, June 2003.

[5] M.J. Jafri, G.D. Pearlson, M. Stevens, and V.D. Calhoun, "A method for functional network connectivity among spatially independent resting-state components in schizophrenia," *NeuroImage*, vol. 39, no. 4, pp. 1666-1681, February 2008.

[6] S.A. Meda, A. Gill, M.C. Stevens, R.P. Lorenzoni, D.C. Glahn, V.D. Calhoun, et al, "Differences in resting-state functional magnetic resonance imaging functional network connectivity between schizophrenia and psychotic bipolar probands and their unaffected first-degree relatives," *Biological Psychiatry*, vol. 71, no. 10, pp. 881-889, May 2012.

[7] Z. Liu, Y. Zhang, L. Bai, Y. Hao, R. Dai, C. Zhong, et al, "Investigation of the effective connectivity of resting state networks in Alzheimer's disease: a functional MRI study combining independent components analysis and multivariate granger causality analysis," *NMR in Biomedicine*, vol. 25, no. 12, pp. 1311-1320, March 2012.

[8] C.C. Abbott, N.T. Lemke, S. Gopal, R.J. Thoma, J. Bustillo, V.D. Calhoun, et al, "Electroconvulsive therapy response in major depressive disorder: a pilot functional network connectivity resting state fMRI investigation," *Frontiers in Psychiatry*, vol. 4, pp. 1-9, March 2013.

[9] M. Kenia, S.A. Beatriz, B. Miguel, H.J. Antonio, J. Álvarez-Linera, F.J. Román, et al, "Changes in resting-state functionally connected parietofrontal networks after videogame practice," *Human Brain Mapping*, vol. 34, no. 12, pp. 3143-3157, December 2013.

[10] S.M. Smith, "The future of FMRI connectivity," *NeuroImage*, vol. 62, no. 2, pp. 1257-1266, August 2012.

[11] E.A. Allen, E.B. Erhardt, E. Damaraju, W. Gruner, J.M. Segall, R.F. Silva, et al., "A baseline for the multivariate comparison of resting-state networks," *Frontiers in Systems Neuroscience*, vol. 5, pp. 1-23. February 2011.

[12] T. Adali and V.D. Calhoun, "Complex ICA of brain imaging data," *IEEE Signal Processing Magazine*, vol. 24, no. 5, pp. 136-139, September 2007.

[13] V.D. Calhoun and T. Adali, "Multi-subject independent component analysis of fMRI: a decade of intrinsic networks, default mode, and neurodiagnostic discovery," *IEEE Reviews in Biomedical Engineering*, vol. 5, pp. 60-73, August 2012.

[14] H. Li, N.M. Correa, P.A. Rodriguez, V.D. Calhoun, and T. Adali, "Application of independent component analysis with adaptive density model to complex-valued fMRI data," *IEEE transactions on bio-medical engineering*, vol. 58, no. 10, pp. 2794-2803, October 2011.

[15] D.B. Rowe, "Modeling both the magnitude and phase of complex-valued fMRI data," *Neuroimage*, vol. 25, no. 4, pp.1310-1324, May 2005.

[16] M.C. Yu, Q.H. Lin, L.D. Kuang, X.F. Gong, F. Cong, and V.D. Calhoun, "ICA of full complex-valued fMRI data using phase information of spatial maps," *Journal of Neuroscience Methods*, vol. 249, pp. 75-91, July 2015.

[17] P.A. Rodriguez, N.M. Correa, T. Eichele, V.D. Calhoun, and T. Adali, "Quality map thresholding for denoising of complex-valued fMRI data and its application to ICA of fMRI," *Journal of Signal Processing Systems*, vol. 65, no. 3, pp. 497-508, September 2011.

[18] P.A. Rodriguez, V.D. Calhoun, and T. Adali, "De-noising, phase ambiguity correction and visualization techniques for complex-valued ICA of group fMRI data," *Pattern Recognition*, vol. 45, no. 6, pp. 2050-2063, June 2012.

[19] X.L. Li, and T. Adali, "Complex independent component analysis by entropy bound minimization," *IEEE Transaction on Circuits and Systems-I: Regular Papers*, vol. 57, no.7, pp.1417-1430, April 2010.

[20] S.M. Smith, P.T. Fox, K.L. Miller, D.C. Glahn, P.M. Fox, C.E. Mackay, et al. "Correspondence of the brain's functional architecture during activation and rest," *Proceedings of the National Academy of Sciences*, vol. 106, no. 31 pp. 13040-13045, August 2009.

[21] A. Bell, and T.J. Sejnowski, "An information-maximization approach to blind separation and blind deconvolution," *Neural Computation*, vol. 7, pp. 1129-1159, December 1995.

[22] L. Rui, J. Yu, S. Zhang, F. Bao, P. Wang, X. Huang, and J. Li, "Bayesian Network Analysis Reveals Alterations to Default Mode Network Connectivity in Individuals at Risk for Alzheimer's Disease," *Plos One*, vol. 8, no. 12, pp. e82104, December 2013.

[23] http://fmri.wfubmc.edu/cms/software.